I&EC research
Industrial & Engineering Chemistry Research

Article

pubs.acs.org/IECR

Optimal Design and Synthesis of Algal Biorefinery Processes for Biological Carbon Sequestration and Utilization with Zero Direct Greenhouse Gas Emissions: MINLP Model and Global Optimization Algorithm

Jian Gong and Fengqi You*

Department of Chemical and Biological Engineering, Northwestern University, Evanston, Illinois 60208, United States

Supporting Information

ABSTRACT: We develop a novel superstructure of algal biorefinery processes for biological carbon sequestration and utilization, encompassing off-gas purification, algae cultivation, harvesting and dewatering, lipid extraction, remnant treatment, biogas utilization, and algal oil upgrading stages. Based on the superstructure, we propose a mixed-integer nonlinear programming (MINLP) model to minimize the unit carbon sequestration and utilization cost and apply a tailored branch-and-refine algorithm based on successive piecewise linear approximation to globally optimize the resulting nonconvex MINLP problem efficiently. The minimum unit carbon sequestration and utilization cost of \$1.48/ton of CO_2 is obtained when the diesel price is \$3.91/gal and feed gas is delivered to the biorefinery only during daytime at a flow rate of 5003.46 ktons/year corresponding to the carbon dioxide emission rate of a 600 MW coal-fired power plant. The resulting algal biorefinery design reuses all the CO_2 produced within the process, leading to zero direct greenhouse gas emission of the entire process.

1. INTRODUCTION

Climate change, a well-recognized fact currently, is critical enough to jeopardize our society and environment. Increasing greenhouse gas (GHG) emissions from human activities such as deforestation and fossil fuel combustion are believed to contribute to most of the climate change. As a result, researchers are seeking every possible method to mitigate side effects of global warming. One of the most important methods involves carbon sequestration, a set of technologies to store carbon dioxide emissions from industrial power plants. Geological injection, oceanic injection, and mineral carbonation have received excessive attention in recent years because of their potentially larger sequestration capacity. However, abiotic sequestration technologies suffer from the risk of unexpected leakage and unstable investment cost depending highly on the geological characteristics of the targeted reservoir. Fortunately, a biological sequestration pathway provides an alternative choice. "Algae" usually refers to a diverse category of organisms which consume carbon dioxide very quickly during photosynthesis and have excellent potential of accumulating lipid materials that can be upgraded to hydrocarbon liquid fuels through transesterification or a hydroprocessing pathway.[1,2] Additionally, algal biofuels largely avoid the competition of arable land with conventional agriculture products. The goal of this work is to use the superstructure optimization method for process design and synthesis to investigate the economic competitiveness of an algal biorefinery as a potential approach for biological carbon sequestration and utilization.

General reviews on technologies involved in the algae-to-biofuel process are given by Brennan et al.,[3] Chisti,[4] and Mata.[5] Some of the recent literature concerned with the process design and synthesis of biomass-based energy systems is reviewed below. Martin and Grossmann studied the optimal algal composition for the simultaneous production of bioethanol and biodiesel[6] and addressed the optimal production of second-generation biodiesel from waste cooking oil and algae oil through five different transesterification technologies.[7] Baliban et al.[8] introduced a superstructure model to convert hardwood biomass to liquid transportation fuels with heat, power, and water integration. The model was solved by applying piecewise linear underestimation and a rigorous global optimization branch-and-bound strategy. Chen et al.[9] investigated the optimal design and operation of flexible energy polygeneration systems to produce power, liquid fuels, and chemicals from coal and biomass. The problem was solved to global optimality by a tailored duality-based decomposition method. Liu et al.[10] proposed a stochastic programming framework for the optimal design under uncertainty of polygeneration energy systems. The mixed-integer nonlinear programming (MINLP) problem was handled by a tailored decomposition algorithm. Gebreslassie et al.[11] built a comprehensive superstructure of an algal biorefinery for hydrocarbon biofuel production and carbon sequestration. Then they solved the proposed multiobjective MINLP problem using a heuristic algorithm and obtained a Pareto-optimal curve which revealed the trade-offs between two objective functions, net present value and global warming potential. Wang et al.,[12] Gebreslassie et al.,[13] and Zhang et al.[14] proposed multiobjective MINLP models for superstructure optimization of a hydrocarbon biorefinery via gasification and pyrolysis pathways. The growing popularity of research into algae cultivation and downstream upgrading spurs the investigation of the techno-

Received: October 14, 2013
Revised: December 20, 2013
Accepted: January 3, 2014
Published: January 3, 2014

dx.doi.org/10.1021/ie403459m | *Ind. Eng. Chem. Res.* 2014, 53, 1563−1579

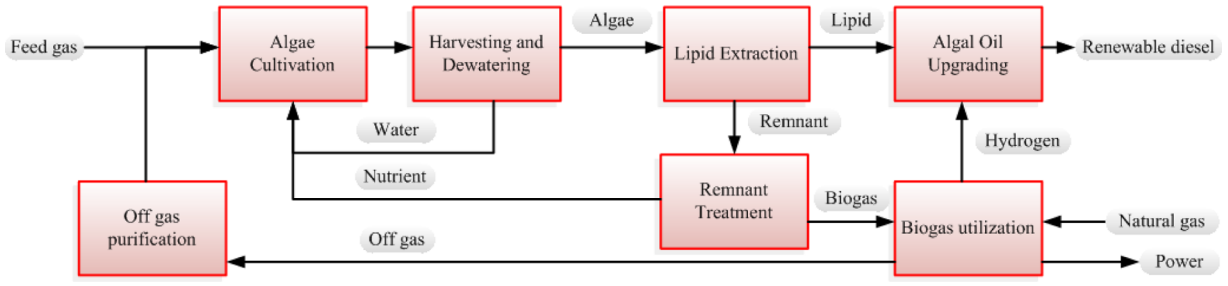

Figure 1. Block flow diagram of the algal biorefinery.

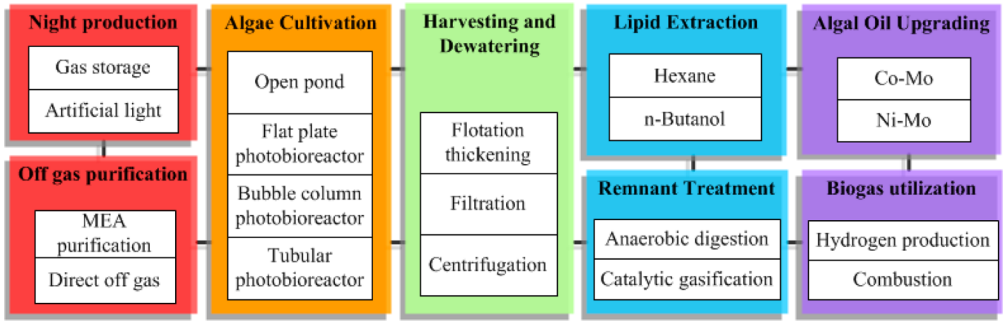

Figure 2. Alternative technologies/processes considered in the superstructure.

logical integration, economic viability, and environmental impact of the algal biorefinery from a process-systems-engineering point of view. Davis et al.[15,16] investigated the baseline economics for two microalgae pathways, and rigorous mass balances were performed using ASPEN PLUS simulation software resulting in production costs of $9.84/gal for open ponds and $20.53/gal for photobioreactors. Frank et al.[17] performed a life cycle analysis of GHG emissions and energy use for algal biofuel production by the GREET model. Special attention was paid to energy recovery through biogas production from the residual biomass after lipid extraction. Pokoo-Aikins et al.[18] addressed the design and technoeconomic analysis of the production of biodiesel from algal oil using ASPEN PLUS simulation and ICARUS cost estimation. Sun et al.[19] estimated the algal oil production cost based on a normalized set of input assumptions from a harmonization study[16] and obtained a range from $10.87/gal to $13.32/gal. Lundquist et al.[20] assessed the economics of microalgae biofuel production through an analysis of five production scenarios and provided recommendations for large-scale algae biofuel production.

Unfortunately, none of the simulation-based works reviewed above considers the technological integration, economic viability, and environmental impact of algal biorefinery processes simultaneously. To the best of our knowledge, very little attention has been paid to algal process topology optimization, which relies on rigorous mathematical modeling and computational techniques to explore the most economically competitive and environmentally friendly design of an algal biorefinery.

In this work, we develop a strengthened process superstructure for biological carbon sequestration and utilization by directly processing wet algae biomass to avoid the intensive energy consumption of complete drying and incorporating a plethora of technology alternatives in off-gas purification, algae cultivation, harvesting and dewatering, lipid extraction, remnant treatment, biogas utilization, and algal oil. The technology alternatives included are direct utilization and purified carbon dioxide by monoethanolamine (MEA) adsorption process for recycled off-gas; open pond and three types of photobioreactors for algae culture; flotation thickening, filtration, and centrifugation to dehydrate algal slurry; hexane and 1-butane as lipid extractants; anaerobic digestion and catalytic gasification to exploit algal remnant; and two catalysts, Co−Mo and Ni−Mo, in hydroprocessing reactors. On the basis of the process superstructure, we formulate a corresponding MINLP model to determine the most economical process design and operation conditions of the algal biorefinery subject to mass balance constraints, energy balance constraints, technoeconomic constraints, and life cycle assessment (LCA) constraints. What is more, we apply a tailored branch-and-refine algorithm based on successive piecewise linear approximation to globally optimize the resulting nonconvex MINLP problem and significantly improve the computational efficiency. The minimum unit carbon sequestration and utilization cost of $1.48/ton of CO_2 sequestrated is obtained when the diesel price is $3.91/gal and feed gas of 99% carbon dioxide by weight is delivered to the biorefinery only during daytime at a flow rate of 5003.46 ktons/year, corresponding to the carbon dioxide emission rate of a 600 MW coal-fired power plant. The optimal process design of this case employs an open pond, flotation thickening, 1-butanol solvent extraction, anaerobic digestion, biogas utilized to produce hydrogen, and Ni−Mo as the catalyst in the algal oil upgrading reactor.

The major novelties of this work are highlighted as follows:

- a new superstructure of algal biorefinery processes for biological carbon sequestration and utilization as well as its corresponding MINLP model for process topology optimization
- a tailored branch-and-refine algorithm to efficiently and globally solve the nonconvex MINLP problems for superstructure optimization
- quantitative analysis to demonstrate the economic competiveness of algal oil production over other mainstream carbon sequestration methods

dx.doi.org/10.1021/ie403459m | Ind. Eng. Chem. Res. 2014, 53, 1563−1579

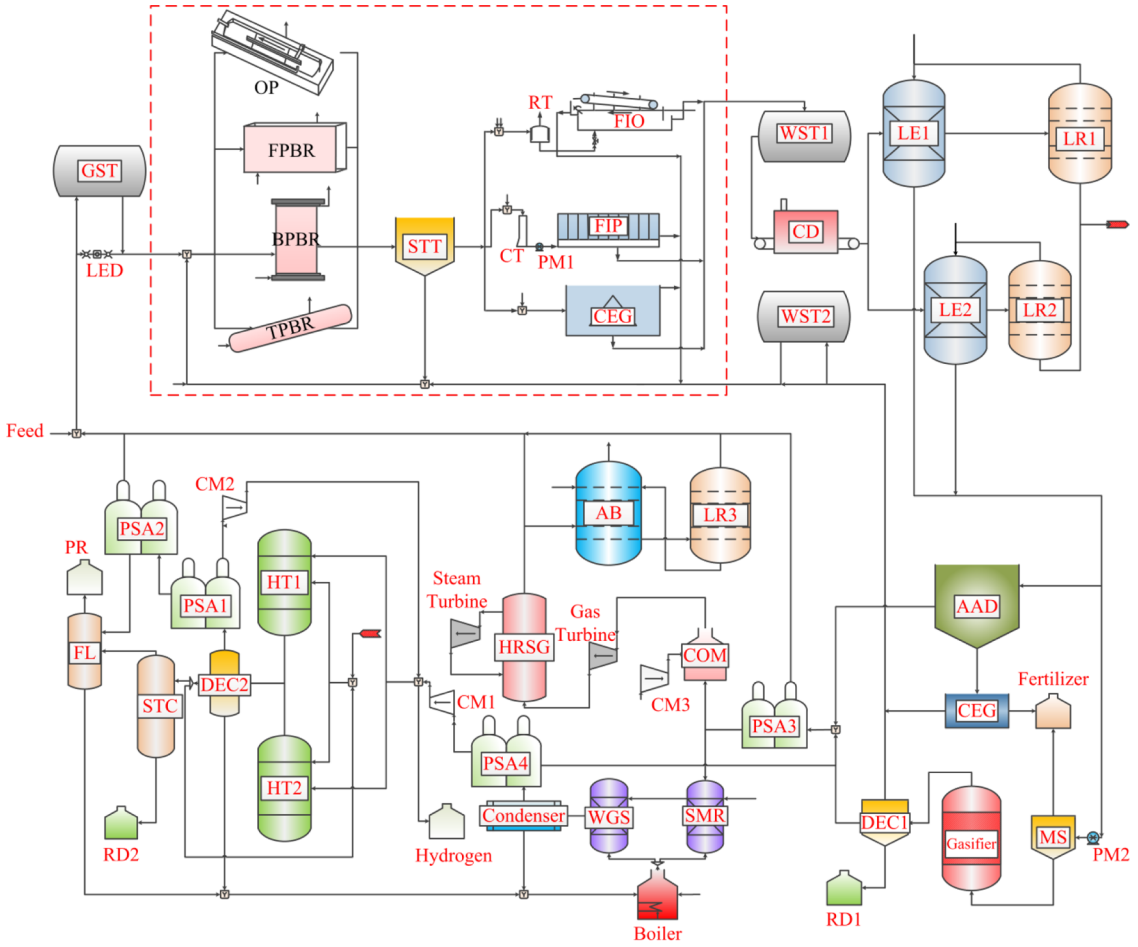

Figure 3. Superstructure of the algal biorefinery for feed gas delivered 24 h a day. GST, gas storage tank; LED, light-emitting diode; OP, open pond; FPBR, flat-plate photobioreactor; BPBR, bubble photobioreactor; TPBR, tubular photobioreactor; STT, sedimentation basin; RT, retention tank; CT, conditioning tank; PM, pump; FIO, flotation thickening; FIP, filtration; CEG, centrifugation; WST, liquid storage tank; CD, cell disruption; LE, lipid extractor; LR, extractant recovery; AAD, anaerobic digestion; MS, mineral separator; DEC, decanter; PSA, pressure swing adsorption; COM, combustor; CM, compressor; HRSG, heat recovery steam generation; AB, monoethanolamine adsorption; SMR, steam reforming; WGS, water gas shift; HT, hydrotreating; STC, distillation column; FL, flash drum; RD, renewable diesel; PR, propane.

The rest of the paper is organized as follows. Process description is presented in section 2. The problem statement is shown in section 3. Section 4 provides a detailed mathematical model formulation. Solution approaches are developed in section 5. Computational results are discussed in section 6. Section 7 gives the conclusion of this work.

2. PROCESS DESCRIPTION

The algal biorefinery for biological carbon sequestration integrated with hydrocarbon production encompasses seven major sections which are highlighted in big red boxes in Figure 1. Namely, they are off-gas purification, algae cultivation, algal harvesting and dewatering, lipid extraction, remnant treatment, biogas utilization, and algal oil upgrading. Each section contains several operation units such as mixers, splitters, pumps, compressors, and stripping columns. For important units, such as reactors and extractors, there are multiple alternative technologies (illustrated in Figure 2) which can be equivalently substituted by any of them, but each has strengths and weaknesses in terms of economics and efficiency. The detailed process flow diagram including all alternative technologies in the case of whole-day feed gas delivery is shown in Figure 3.

2.1. Off-Gas Purification. In order to cultivate enough algae in bioreactors for downstream processing, a large quantity of carbon dioxide is necessary as the main feedstock for the entire biofuel production. Here we make an assumption that a coal-fired power plant nearby has a set of MEA equipment to separate the CO_2 from flue gas. The composition of this post-carbon-capture feed gas is listed in Table 1, as reported by Fisher et al.[21]

Table 1. Gaseous Composition of Feed Gas

constituent	weight fraction (%)
water	1
carbon dioxide	99

The goal of this biorefinery is to sequester the carbon dioxide and convert it into value-added products. As shown in Figure 3, all of the carbon dioxide produced within the process is recycled back as the feed for algal growth including the off-gas from the heat recovery steam generation (HRSG) system. If combustion is selected to deal with the biogas following the remnant treatment section, the resulting off-gas will be a mix of nitrogen, carbon dioxide, oxygen, and water. However, carbon dioxide is the only effective constituent in algae photosynthesis and it makes up only a small proportion. One easy option is that the off-

dx.doi.org/10.1021/ie403459m | Ind. Eng. Chem. Res. 2014, 53, 1563−1579

gas can be fed to bioreactors directly, which will lower the productivity and increase the storage expense significantly. On the other hand, the combination of MEA adsorption and a recovery stripping column[21] is able to separate carbon dioxide from off-gas but inevitably causes high investment and operating costs. Note that surplus water content in the off-gas feed does not dilute the MEA adsorbent or affect its efficacy because, according to Fisher et al.,[21] phase equilibrium suggests no steam in the feed gas condenses under the operating condition and even more water is replenished to account for the slight evaporation in the MEA adsorbent. After adsorption, all waste species, namely water, nitrogen, and oxygen, are released from the top of the absorber.

2.2. Algae Cultivation. After feed gas is enriched by reusable carbon dioxide and fed to bioreactors together with water and nutrients, algae are able to grow in the presence of light. Before bioreactors are selected for algae, the algae species itself is a problem to address with priority. The term "algae" actually refers to a diverse cluster of organisms from different living habits.[1] According to the review by Mata et al.,[5] many species exhibit surprising potentials with respect to lipid accumulation and the best lipid weight fraction ever found is as high as 70% of the algae dry weight. Even though high lipid accumulation is achieved, researchers are still attempting to find and culture more suitable algae species for industrial production by genetic engineering methods. In this work, we choose the microalga *Phaeodactylum tricornutum*[5,22] to grow in the bioreactors and make two assumptions about it: (1) the lipid content reaches 25% of its dry weight; (2) it is able to survive in any type of bioreactor for enough time to reach the intended concentration level.[16]

Algal bioreactors received extensive attention in the past 20 years, and much comparison and analysis was made among different types of bioreactors.[23−28] Nevertheless, no consensus is drawn on which one is the most effective and efficient because each one has its strengths and weaknesses. Despite disagreement about the best option, most researchers would agree that an open pond, especially a raceway reactor for algae growth, is relatively less expensive in terms of construction and operation. However, the open pond might be less productive than closed photobioreactors and it may be easily contaminated by external microbes and affected by bad weather conditions. Closed photobioreactors generally tend to show high productivity and high resistance to the external weather conditions. However, they might be expensive to build and operate. In the process superstructure, we consider four alternatives: open pond, flat plate photobioreactor, bubble column photobioreactor, and tubular photobioreactor. When algae grow in the bioreactors, they consume carbon dioxide, nutrients, and water, accumulate biomass, and release oxygen. Unfortunately, the excessive dissolved oxygen in the algal cultures inhibits high photosynthetic efficiency. As a result, closed photobioreactors are designed with limited length and airlift systems every few meters to control oxygen concentration; for the open pond, oxygen is directly emitted to the atmosphere.

One big issue about algae growth conditions is the light supply, because light is the major energy source for algae to perform photosynthesis.[29] Free sunlight radiation is available only during daytime, so it naturally becomes a critical decision whether to provide an artificial light source after sunset or to store all the feed gas for algae production in the next day. If gas storage is selected, two more tanks will be employed to hold extra algae slurry and recycled water so that the entire biorefinery is manually partitioned into two areas, continuous and discontinuous, the border of which is highlighted by the red dashed box in Figure 3.

2.3. Harvesting and Dewatering. The mature algae from the open pond or photobioreactor are considerably dilute, which is not qualified for downstream upgrading directly. For the purpose of dehydration, several techniques are employed. As a preliminary settling device, a sedimentation basin is capable of concentrating algae slurry to 1%.[11] However, it is not the acceptable range for wet lipid extraction. Thus one advanced dehydration technology, flotation thickening, filtration, or centrifugation, is required to further reduce moisture. Flotation thickening is poor in the dewatering effect, but it consumes less energy. Filtration and centrifugation are both able to dry the solid content effectively at an intensive energy cost. To maximize the resource utilization, split water from the above two-step dewatering section is sent back to bioreactors as nutrients for algae nourishing.

2.4. Lipid Extraction. Most chemical plants operate continuously for a long time and shutdowns appear only when regular maintenance, unexpected failures, and process facilities upgrading happen. This is because frequent shutdowns and startups definitely jeopardize the mechanical stability of devices and incur large quantities of nonprofitable off-spec products during transition. In our superstructure, the discontinuous section is highlighted as the red dashed box in Figure 3 if gas storage by gasholders at night is selected. All of the downstream processes are designed to be continuous and a storage tank is arranged to reserve concentrated algae slurry for cell disruption at night.

After the joint storage tank, intracellular lipid, the precursor of biofuel, is separated from the algae cell by solvent extraction. However, the existence of algal biological features such as cell wall and cell membrane physically prevent the contact of solvent with lipid materials. As a result, cell disruption is an essential step prior to the lipid extraction process. Here, we take advantage of the existing investigation[30,31] and choose microwave radiation as the intended disruption method because it is the most effective and energy efficient method compared with others.

Solvent extraction is a common unit operation in the chemical industry. The choice of solvent depends on the properties of material extracted as well as demanding operation conditions. Here for lipid extraction we consider two options: hexane and 1-butanol.[32] Hexane outweighs 1-butanol in terms of lower boiling point, lower water miscibility, and lower purchase cost, but its drawback lies in lower extraction effect and larger facility capacity due to higher solvent to biomass ratio. We retrieve the extraction and distillation parameters directly from the literature.[15,32]

2.5. Remnant Treatment. One of the potentially greatest amounts of waste in the context is the algae remnant, which is the remaining cell body after lipid extraction. One option to handle the algae remnant is anaerobic digestion,[33] which would produce biogas typically consisting of about 40% carbon dioxide and 60% methane by volume, a liquid effluent rich in soluble nutrition for algae cultivation, and solid waste to sell as farming fertilizer. The alternative is to employ catalytic gasification, which according to Elliott et al.[34] is reported to produce biogas consisting of 0.5% ethane, 2.1% hydrogen, 38% carbon dioxide, and 57.1% methane, a solid rich in mineral deposits, an aqueous product with nitrogen and phosphorus nutrition, and most surprisingly an oil product which can be regarded as renewable diesel.

2.6. Biogas Utilization. Biogas produced by either anaerobic digestion or catalytic gasification can be utilized directly on site. We consider two utilization technologies: combustion and steam

reforming. Biogas combustion process encompasses an air compressor, a combustor, a gas turbine, and a HRSG subsystem. After biogas is burned with adequate pressurized air in the combustor, the energy of the hot flue gas is converted to electricity in both the gas turbine and the HRSG. The total efficiency for heat and power recovery is set as 76% on a lower heating value (LHV) basis.[17] Additionally, off-gas from the HRSG subsystem is able to serve as supplementary feed gas since the composition is nearly identical to flue gas from a power plant. On the other hand, if biogas from upstream was sequentially sent to steam reforming and water gas shift reactors to assist hydrogen production,[35] the natural gas purchase cost would be largely reduced, but power consumption for other sections should be satisfied by an outside supply. Note that whatever the upstream process is, the reports[33,34] indicate no contaminating acid gas species emerging from remnant treatment, but if H_2S or other acid gas is mixed in the biogas, extra process units are necessary to further purify this waste acid gas.

2.7. Algal Oil Upgrading. The last section of this process is algal oil upgrading. A large proportion of algal lipids is made up of triacylglycerides (TAGs), and two major pathways currently are able to convert TAGs to diesel.[36] One is referred to as transesterification and the reaction results in fatty acid methyl esters (FAMEs), or so-called biodiesel. On the other hand, TAGs, FAMEs, or free fatty acids (FFAs) are able to undergo deoxygenation and obtain saturated hydrocarbons with other coproducts depending on the specific mechanism. A hydrocarbon from such pathway does not contain an oxygen atom, and this product is usually known as renewable diesel or green diesel. Judged from the facts of oxygen existence, biodiesel is less stable and compatible for blending with petroleum based diesel than renewable diesel. Additionally, the transesterification mechanism requires algal lipids to be free of FFAs to avoid producing fatty acid salts or soaps which will unfortunately reduce product quality and plug related devices. Furthermore, transesterification has been discussed extensively in the literature, so we only focus on deoxygenation mechanisms in this work.

There are two major deoxygenation pathways: one is hydrodeoxygenation, which produces hydrocarbons and water with the participation of hydrogen, and the other one is decarboxylation, which straightly eliminates oxygen atoms by formulating carbon dioxide and saves hydrogen consumption. According to Marker et al.[37] there is no clear boundary for the present two mechanisms, but a dominant mechanism is recognized for different catalysts. On the basis of their report, we choose Co−Mo catalyst for the decarboxylation mechanism and Ni−Mo for the hydrodeoxygenation mechanism as two alternatives in the superstructure. The rest of the layout of this section is similar to the superstructure of Gebreslassie et al.[11]

2.8. Zero Direct GHG Emissions. The main purpose of establishing this algal biorefinery is to sequestrate carbon dioxide emissions from upstream coal-fired power plants, so the process superstructure needs assessments from both the sequestration and economic perspectives. In terms of the sequestration effect, it is not difficult to identify that there are two streams discharging waste gases directly into the atmosphere. One is the oxygen stream produced from algae cultivation; the other is purified off-gas stream from the MEA process which contains nitrogen, oxygen, water, and a small amount of carbon dioxide. If the direct off-gas pathway is selected, which is the case for all of our optimal results, our algal biorefinery consumes all GHG from both external and internal sources. In other words, this algal biorefinery has zero direct GHG emissions.

3. PROBLEM STATEMENT

In this work, we are given the specific superstructure configuration of an algal biorefinery for biological carbon sequestration and hydrocarbon production from carbon dioxide produced by the upstream coal-fired power plant. Properties of the feed gas including the mass flow rate and composition are known. The split fraction of each species in separation equipment and operating conditions of similar equipment are retrieved from similar works. Other given parameters include the following:

- hours of sun light during the day
- scale coefficients of each species in MEA based on feed carbon dioxide
- unit consumption of necessary species in algae cultivation
- productivities of various types of bioreactors during the day
- LED intensity choices and corresponding productivities during and night
- algae concentration in the product stream of each type of bioreactor
- concentration of major species in makeup extraction solvents
- product distribution of anaerobic digestion and catalytic gasification
- concentrations of nutrients in the aqueous phase of anaerobic digestion and catalytic gasification
- excess air feed for biogas combustion
- stoichiometric ratios of products over one reactant in combustion
- conversion of each reactant in steam reforming reactor
- molar ratio of steam over carbon and conversion in water gas shift reaction
- unit hydrogen consumption for each type of catalyst in hydrotreating reactor
- product distribution of hydrotreating reactor
- temperature difference of each species in condenser
- molecular weight, density, heat capacity, lower heating value of species
- unit heat and power consumption of process equipment
- energy efficiency of gas turbine and steam turbine system
- base case costs and mass flow rates of process equipment
- cost sizing factors
- chemical engineering plant cost index
- market price of power, steam, monoethanolamine, nutrients, water, polymer in dewatering, extractant, natural gas, catalyst, hydrogen, renewable diesel, propane, and fertilizer
- percentage of equipment installation cost, instrument and control cost, piping cost, electrical systems cost, buildings plus services cost, engineering cost, construction cost, legal and contractors cost, project contingency cost, land cost, and working capital cost on the basis of equipment purchase cost
- life span of the biorefinery
- interest rate
- damage factor of the direct emissions
- unit GWP contribution of power and heat

Major assumptions involved in the model formulation are the following:

- Linear relationships are applied between the feed mass flow rate and heat and power consumption regarding relevant equipment.

dx.doi.org/10.1021/ie403459m | Ind. Eng. Chem. Res. 2014, 53, 1563−1579

- All recycled water and carbon dioxide can be directly utilized.
- The operating temperature of the water gas shift reactor is 155 °C.

The goal of this problem is to determine the optimal process design and operation conditions of the algal biorefinery by minimizing the total carbon sequestration and utilization cost, subject to mass balance constraints, energy balance constraints, technoeconomic evaluation constraints, and life cycle environmental impact constraints. The major decision variables include the following:

- technology selection
- mass flow rate of each species in every stream
- heat and power consumption of each piece of equipment
- capital cost and operating cost required for economic evaluation
- environmental impacts

4. MODEL FORMULATION

The mathematical model is formulated as an MINLP problem which simultaneously determines the optimal design and operation conditions of the algal biorefinery for biological carbon sequestration and utilization at the minimum cost. The MINLP model involves four major types of constraints, which are mass balance constraints (S1)−(S122), energy balance constraints (S123)−(S126), economic evaluation constraints (1)−(18), and gate-to-gate life cycle environmental impact constraints (19)−(23). In this model, the objective function is defined as (18), which is the biological carbon sequestration and utilization cost per unit mass of carbon dioxide sequestrated.

The MINLP model includes one bilinear term in (S32) to quantify the volume of the bioreactor. Furthermore, some nonconvex nonlinear terms appear in the economic analysis constraints, which contain a number of capital cost evaluation equations in (4)−(9).

In order to help focus on the essence of this work, the detailed mass balance and energy balance constraints are given in the Supporting Information. Details about the economic analysis constraints and life cycle environmental impact constraints are shown in sections 4.1 and 4.2.

4.1. Economic Analysis Constraints. The target of economic analysis is to identify the total annualized cost, including capital cost and operating cost, per unit mass of carbon dioxide sequestrated in the optimal design. Capital costs for gasholders, water storage tanks,[38] and sediment basin[39] are given in (1)−(3). In these relationships, $\text{Price}_{\text{gasholder}}$ and $\text{Price}_{\text{cone roof}}$ are prices for a gasholder and a cone-roof tank, respectively; V^{gas} and V^{wr} are maximum container volumes in the market; T_{time} is the time duration and ρ_{jdfg} is the density of species jdfg; $\text{Unitprice}_{\text{basin}}$ and $\text{Unitprice}_{\text{drainage}}$ are unit prices of the sediment basin and drainage respectively; t is the settling time; and h_{basin} is the height of the basin.

$$\text{CC}_{\text{gst}} = \text{Price}_{\text{gasholder}} \sum_{\text{jdfg}\in\{\text{wr},\text{cdo},\text{nit},\text{oxy}\}} \frac{T_{\text{night}} m^{\text{fg2,night}}_{\text{gst,jdfg}}}{\rho_{\text{jdfg}} V^{\text{gas}}} \tag{1}$$

$$\text{CC}_{\text{wst}} = \text{Price}_{\text{cone roof}} \sum_{j\in J} \frac{T_{\text{day}}(m^{\text{ca}}_{\text{day},j} - m^{\text{cdf}}_{j}) + T_{\text{night}} m^{\text{ntf}}_{\text{gst},j}}{\rho_{\text{wr}} V^{\text{wr}}} \tag{2}$$

$$\text{CC}_{\text{st}} = \text{Unitprice}_{\text{basin}} \sum_{j\in J} m^{\text{as}}_{\text{day},j} t + \text{Unitprice}_{\text{drainage}} \frac{\sum_{j\in J} m^{\text{as}}_{\text{day},j} t}{h_{\text{basin}}} \tag{3}$$

Capital costs for flotation thickening, filtration, centrifugation, anaerobic digestion, and decanters follow empirical equations (4)−(8), where $\text{Uni}^{\text{m3,gal}}$ is the unit converter from cubic meter to gallon.[11]

$$\text{CC}_{\text{flo}} = 0.0904 \left(\sum_{j\in J} \frac{24 m^{\text{dwf}}_{\text{day,flo},j} \text{Uni}^{\text{m3,gal}}}{\rho_{\text{wr}}} \right)^{1.14} \tag{4}$$

$$\text{CC}_{\text{fil}} = 0.099 \left(\sum_{j\in J} \frac{24 m^{\text{dwf}}_{\text{day,fil},j} \text{Uni}^{\text{m3,gal}}}{\rho_{\text{wr}}} \right)^{0.4535} \tag{5}$$

$$\text{CC}_{\text{ceg}} = 0.099 \left(\sum_{j\in J} \frac{24 m^{\text{dwf}}_{\text{day,ceg},j} \text{Uni}^{\text{m3,gal}}}{\rho_{\text{wr}}} \right)^{0.574} + 0.099 \left(\sum_{j\in J} \frac{24 (m^{\text{fer}}_{\text{aad},j} + m^{\text{rnt}}_{j}) \text{Uni}^{\text{m3,gal}}}{\rho_{\text{wr}}} \right)^{0.574} \tag{6}$$

$$\text{CC}_{\text{aad}} = 0.0001849 \left(\sum_{j\in J} m^{\text{rtf}}_{\text{aad},j} \right)^{0.472} \tag{7}$$

$$\text{CC}_{\text{dec}} = 0.0918 \left(\sum_{j\in J} \frac{24 (m^{\text{wr 31}}_{j} + m^{\text{wr 31}}_{j} + m^{\text{gd21}} + m^{\text{gd22}}) \text{Uni}^{\text{m3,gal}}}{\rho_{\text{wr}}} \right)^{1.1} + 0.0918 \left(\sum_{\text{htt}\in\text{HTT}, j\in J} \frac{24 m^{\text{hps}}_{\text{htt},j} \text{Uni}^{\text{m3,gal}}}{\rho_{\text{wr}}} \right)^{1.1} \tag{8}$$

Capital cost evaluation for other units l3 are given by the size exponent method as shown in eq 9, where $\text{CC}^{\text{b}}_{\text{l3}}$ is the capital cost of unit l3 in the base case, f^{b}_{l3} is the total effect inlet flow of unit l3 in the base case, and sf_{l3} is the sizing factor[11] of unit l3. Furthermore, we use the chemical engineering plant cost index[40] to account for inflation of the capital cost from the reference year.

$$\text{CC}_{\text{l3}} = \text{CC}^{\text{b}}_{\text{l3}} \left(\frac{\sum_{j\in J} m_{\text{l3},j}}{f^{\text{b}}_{\text{l3}}} \right)^{\text{sf}_{\text{l3}}} \left(\frac{\text{CEPCI}_{\text{l3}}}{\text{CEPCI}^{\text{ref}}_{\text{l3}}} \right), \qquad \forall\ \text{l3} \in \text{L3} \tag{9}$$

$$\text{L3} = \{\text{ab, op, bpbr, fpbr, tpbr, cd, pump, compressor1, compressor2, compressor3, psa1, psa2, psa3, psa4, dis1, dis2, flash, gt, le, gas, hyp, str}\}$$

Then the total investment cost (TIC) of this biorefinery is given as the sum of all equipment costs, engineering cost (K_{eng}), legal and contractors cost (K_{lg}), project contingency cost (K_{ctg}), and working capital cost (K_{wcp}), as well as land cost. All these costs except land cost are calculated as a percentage of the total equipment cost. Unitland is the unit land cost; $\text{areapro}_{\text{agt}}$ is the areal productivity of technology agt.

dx.doi.org/10.1021/ie403459m | Ind. Eng. Chem. Res. 2014, 53, 1563−1579

$$\mathrm{TIC} = \sum_{l\in L} \mathrm{CC}_l(1 + K_{\mathrm{eng}} + K_{\mathrm{lg}} + K_{\mathrm{ctg}} + K_{\mathrm{wcp}}) + 1.5\mathrm{Unitland} \sum_{\mathrm{agt}\in\{\mathrm{op,fpbr,bpbr,tpbr}\}} \sum_{\mathrm{cct}\in\{\mathrm{afg,dfg}\}} \sum_{\mathrm{time}\in\mathrm{TIME}} \frac{m^{\mathrm{agp}}_{\mathrm{agt,cct,time},j}}{\mathrm{areapro}_{\mathrm{agt}}} \quad (10)$$

L = {ab, gst, op, bpbr, fpbr, tpbr, st, flo, fil, ceg1, ceg2, wst, cd, pump, compressor1, compressor2, compressor3, psa1, psa2, psa3, psa4, dis1, dis2, flash, gt, le, aad, gas, hyp, str}

As defined by eq 11, the annualized investment cost (AIC) is given by distributing the entire investment cost uniformly in the life span of the biorefinery. ir is the interest rate and lifespan is the life span of the biorefinery. The set

L4 = {MEA, P, N, wr , chf, ext, ng, cata}

$$\mathrm{AIC} = \mathrm{TIC}\cdot\mathrm{ir}\cdot(\mathrm{ir}+1)^{\mathrm{lifespan}-1}/((\mathrm{ir}+1)^{\mathrm{lifespan}}-1) \quad (11)$$

$$\mathrm{FPC} = \sum_{\mathrm{l4}\in\mathrm{L4}} \mathrm{Price}_{\mathrm{l4}} m_{\mathrm{l4}} \quad (12)$$

$$\mathrm{STMC} = \mathrm{Price}_{\mathrm{stm}}\Big(\sum_{\mathrm{l1}\in\mathrm{L1}} Q_{\mathrm{c}}^{\mathrm{l1}} - Q_{\mathrm{g}}\Big) \quad (13)$$

$$\mathrm{PC} = \mathrm{Price}_{E}\Big(\sum_{\mathrm{l2}\in\mathrm{L2}} E_{\mathrm{c}}^{\mathrm{l2}} - E_{\mathrm{g}}\Big) \quad (14)$$

$$\mathrm{OMC} = K_{\mathrm{OM}}\mathrm{AIC} \quad (15)$$

$$\mathrm{AOC} = \mathrm{FPC} + \mathrm{STMC} + \mathrm{PC} + \mathrm{OMC} \quad (16)$$

The annual operating cost (AOC) is evaluated as the sum of the feed purchasing cost (FPC), steam cost (STMC), and power cost (PC) along with the operation and maintenance cost (OMC) as given in (12)−(16), where Price_j is the unit price for species j and K_{OM} is the percentage for the operation and maintenance cost based on the annualized investment cost.

$$\mathrm{TAC} = \mathrm{AIC} + \mathrm{AOC} \quad (17)$$

The total annualized cost (TAC) is determined as the sum of annualized investment cost and the annual operating cost in eq 17. Finally, the objective function (18) is formulated as the actual annual sequestration and utilization cost divided by the total carbon dioxide sequestrated in the whole year. The actual annual sequestration and utilization cost is defined by the total annualized cost minus the revenue from selling all products, including renewable diesel, propane, extra hydrogen, and fertilizer. These products are treated as the credits of the algal biorefinery for biological carbon sequestration.

$$\mathrm{OBJ} = \frac{\mathrm{TAC} - \sum_{\mathrm{l5}\in\mathrm{L5}} \mathrm{Price}_{\mathrm{l5}} m_{\mathrm{l5}}}{\mathrm{pm}^{\mathrm{feed}}_{\mathrm{cdo}}} \quad (18)$$

where the set

L5 = {diesel, propane, hydrogen, fer}

4.2. Life Cycle Environmental Impact Constraints. In the superstructure-optimization model, the environmental footprint of this algal biorefinery is assessed following the principles of LCA, which is a widely used technique to evaluate the environmental impact of a product, process, or service and consists of four phases: goal definition and scoping, inventory analysis, impact assessment, and interpretation. A "gate-to-gate" LCA is conducted dynamically in the superstructure optimization concerning direct emissions during the operation of the algal biorefinery as well as indirect emission resulting from the heat and power consumptions. Direct GHG emissions account for the environmental impact by the two discharging; heat and power are essential for the process and inevitably contribute to the indirect life cycle inventory of the algal biorefinery. We choose GWP as the metric of LCA with a time horizon of 100 years. GWP is a relative scale which compares the global warming influence of a chemical with the global warming impact incurred by the same mass of carbon dioxide whose GWP is 1 by convention.

The GWP of the entire biorefinery encompasses three categories: environmental impact resulting from direct emission ($\mathrm{GWP}^{\mathrm{de}}$), environmental impact caused by power consumption ($\mathrm{GWP}^{\mathrm{pc}}$), and environmental impact contributed by heat consumption ($\mathrm{GWP}^{\mathrm{hc}}$).

$$\mathrm{LCI}_j^{\mathrm{emiss}} = \mathrm{LCI}_j^{\mathrm{w1}} + \mathrm{LCI}_j^{\mathrm{w2}} \quad (19)$$

$$\mathrm{GWP}^{\mathrm{de}} = \sum_{j\in J} \phi_j \mathrm{LCI}_j^{\mathrm{emiss}} \quad (20)$$

In order to quantify the environmental impact resulting from direct emission, life cycle emission inventories are given in eq 19. The algal biorefinery generally has two emission streams, namely, waste gas from off-gas purification, w1, and degassing stream from bioreactor, w2. Then these emissions are converted to GWP contribution by the sum of all products of the damage factor ϕ_j and the corresponding life cycle inventory for each species j as shown in eq 20.

$$\mathrm{GWP}^{\mathrm{pc}} = \theta^{\mathrm{pc}}\Big(\sum_{\mathrm{l2}\in\mathrm{L2}} E_{\mathrm{c}}^{\mathrm{l2}} - E_{\mathrm{g}}\Big) \quad (21)$$

The power consumption contribution is calculated by eq 21, where θ^{pc} is the unit damage factor to describe the environmental influence by producing electricity and $\sum_{\mathrm{l2}\in\mathrm{L2}} E_{\mathrm{c}}^{\mathrm{l2}} - E_{\mathrm{g}}$ is used to account for the net electricity purchased from the utility market. A similar calculation scheme goes for the heat consumption contribution.

$$\mathrm{GWP}^{\mathrm{hc}} = \theta^{\mathrm{hc}}\Big(\sum_{\mathrm{l1}\in\mathrm{L1}} Q_{\mathrm{c}}^{\mathrm{l1}} - Q_{\mathrm{g}}\Big) \quad (22)$$

$$\mathrm{GWP} = \mathrm{GWP}^{\mathrm{de}} + \mathrm{GWP}^{\mathrm{pc}} + \mathrm{GWP}^{\mathrm{hc}} \quad (23)$$

The total GWP indicator is measured via eq 23, and it is the sum of the above three contributions. Although a full-scale life cycle optimization approach[41−43] is not considered in this work, the "gate-to-gate" life cycle environmental impact of this process is considered as constraints for the total direct and indirect life cycle environmental impact analysis which is given later in section 6.

5. SOLUTION APPROACHES

The entire superstructure optimization model is formulated as a nonconvex MINLP problem (P1).

dx.doi.org/10.1021/ie403459m | Ind. Eng. Chem. Res. 2014, 53, 1563−1579

$$\min_{x,y} \quad \text{OBJ given in (18)}$$

s.t. mass balance constraints (S1)−(S27), (S29)−(S122)

energy balance constraints (S123)−(S126)

economic evaluation constraints (1)−(18)

environmental impact constraints (19)−(23)

(P1)

Most of the constraints in the current model are linear conservation relationships. The nonlinear terms appear as one bilinear term in (S32) in the Supporting Information and power functions in the capital cost evaluation, (4)−(9). When the exponents are between 1 and 0, power functions are concave. Otherwise, they are convex. We present the solution strategy of this nonconvex MINLP problem in section 5.1.

5.1. Model Reformulation and Relaxation. *5.1.1. Linearization of the Bilinear Term.* According to Glover,[44] if a bilinear function is made up by the product of a nonnegative continuous variable and a binary variable, this function can be linearized by introducing an auxiliary variable, a big-*M* parameter, and auxiliary constraints. To linearize the nonlinear terms in eq S32 in the Supporting Information, we first convert (S32) to (24) according to the definition of the productivity at night in (S29) in the Supporting Information.

$$\sum_{\text{cct}\in\{\text{afg,dfg}\}} m^{\text{agp}}_{\text{agt,cct,night,al}} \le \text{pproductivity}^{\text{night}}_{\text{agt,ip}} \text{yprod}_{\text{agt,ip}} V_{\text{agt}},$$

$$\forall\ \text{agt} \in \{\text{op, fpbr, bpbr, tpbr}\} \tag{24}$$

Next we replace the bilinear term $\text{yprod}_{\text{agt,ip}} V_{\text{agt}}$ with a nonnegative variable $\omega_{\text{agt,ip}}$ as in (25). Equations 25−28 ensure only one of the discrete points of each bioreactor is active and the reformulation is linear.

$$\sum_{\text{cct}\in\{\text{afg,dfg}\}} m^{\text{agp}}_{\text{agt,cct,night,al}} \le \sum_{\text{ip}\in\text{IP}} \text{pproductivity}^{\text{night}}_{\text{agt,ip}} \omega_{\text{agt,ip}},$$

$$\forall\ \text{agt} \in \{\text{op, fpbr, bpbr, tpbr}\} \tag{25}$$

$$\omega_{\text{agt,ip}} \le V_{\text{agt}}, \qquad \forall\ \text{agt} \in \{\text{op, fpbr, bpbr, tpbr}\},\ \text{ip} \in \text{IP} \tag{26}$$

$$0 \le \omega_{\text{agt,ip}} \le \text{UB}\cdot\text{yprod}_{\text{agt,ip}},$$

$$\forall\ \text{agt} \in \{\text{op, fpbr, bpbr, tpbr}\}, \quad \text{ip} \in \text{IP} \tag{27}$$

$$\omega_{\text{agt,ip}} \ge V_{\text{agt}} - \text{UB}(1 - \text{yprod}_{\text{agt,ip}}),$$

$$\forall\ \text{agt} \in \{\text{op, fpbr, bpbr, tpbr}\}, \quad \text{ip} \in \text{IP} \tag{28}$$

5.1.2. Piecewise Linear Approximation. One typical concave term is the power function in eq 5 with the exponent of 0.4535.

$$\text{CC}_{\text{fil}} = 0.099\left(\sum_{j\in J} \frac{24 m^{\text{dwf}}_{\text{day,fil},j} \text{Uni}^{\text{m3,gal}}}{\rho_{\text{wr}}}\right)^{0.4535}$$

As shown in Figure 4, the nonlinear function can be approximated by a piecewise linear function with four line segments corresponding to three added partition points. Owing to the concave property of the original function, this piecewise function locates closely beneath the power function resulting in

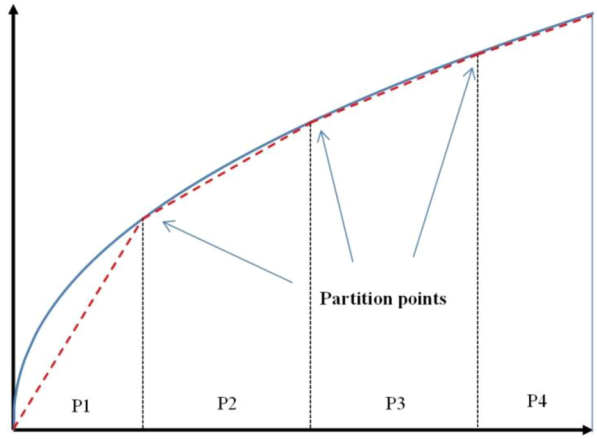

Figure 4. Illustration of concave function lower bounded by piecewise linear function.

an underestimation approximation. In this work we use the "multiple-choice" formulation to model this piecewise linear approximation function.[45,46] As an example, eq 5 can be approximated using the constraints below:

$$\text{CC}_{\text{fil}} = \sum_{p\in P} a_p w_p + b_p y_p \tag{29}$$

$$\sum_{p\in P} y_p = 1 \tag{30}$$

$$\sum_{p\in P} w_p = \sum_{j\in J} \frac{24 m^{\text{dwf}}_{\text{day,fil},j} \text{Uni}^{\text{m3,gal}}}{\rho_{\text{wr}}} \tag{31}$$

$$\text{pp}_{p-1} y_p \le w_p \le \text{pp}_p y_p, \qquad \forall\ p \in P \tag{32}$$

$$y_p \in \{0, 1\}, \quad w_p \ge 0 \qquad \forall\ p \in P \tag{33}$$

$$a_p = \frac{0.099(\text{pp}_p)^{0.4535} - 0.099(\text{pp}_{p-1})^{0.4535}}{\text{pp}_p - \text{pp}_{p-1}},$$

$$b_p = 0.099(\text{pp}_p)^{0.4535} - a_p \text{pp}_p \qquad \forall\ p \in P \tag{34}$$

where set P denotes the intervals in the piecewise function CC_{fil}; pp_p is the upper bound of w_p in the interval p. The rest of the concave power functions are linearized and approximated in the same way.

One typical convex nonlinear term in the objective function is the power function with exponent 1.14 in eq 4.

$$\text{CC}_{\text{flo}} = 0.0904\left(\sum_{j\in J} \frac{24 m^{\text{dwf}}_{\text{day,flo},j} \text{Uni}^{\text{m3,gal}}}{\rho_{\text{wr}}}\right)^{1.14}$$

For the sake of deriving an underestimation of the convex problem, we apply piecewise linear approximation with multiple tangents[47] and the formulation illustrated in Figure 5 is given as follows:

$$\text{CC}_{\text{flo}} \ge 0.0904(\text{pp}_p)^{1.14} + 0.1031(\text{pp}_p)^{0.14}\left(\sum_{j\in J} \frac{24 m^{\text{dwf}}_{\text{day,flo},j} \text{Uni}^{\text{m3,gal}}}{\rho_{\text{wr}}} - \text{pp}_p\right), \qquad \forall\ p \in P \tag{35}$$

dx.doi.org/10.1021/ie403459m | Ind. Eng. Chem. Res. 2014, 53, 1563−1579

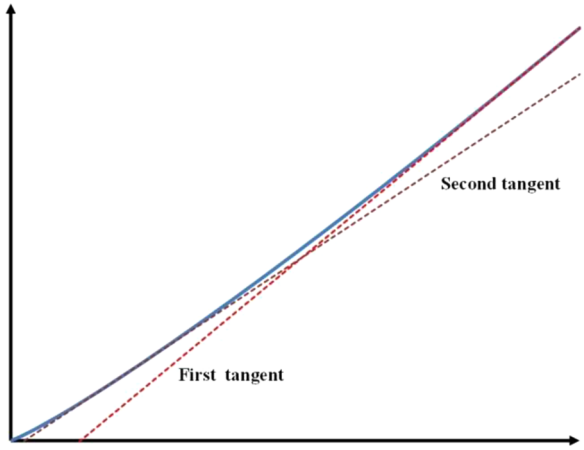

Figure 5. Illustration of convex function lower bounded by piecewise linear function.

where set P denotes the partition point in the piecewise function CC_{flo}; pp_p is the value of the partition point at p. Following a similar relaxation procedure, the remaining convex power functions are underestimated via the piecewise linear approximation of the original nonlinear functions.

5.1.3. Relaxed Problem. As a result of the above linearization transformation techniques, a mixed-integer linear programming (MILP) model (P2) can be formulated as a linear underestimator of the original model (P1) as shown below. Since all constraints for the mass balance and energy balance are reformulated equivalently, the feasible region for both models is the same. We utilized this advantage of the relaxed model and applied a branch-and-refine algorithm to globally optimize the problem. The details are explained in section 5.2.

$$\begin{aligned} \min_{x,y} \quad & \text{OBJ given in (18)} \\ \text{s.t.} \quad & \text{mass balance constraints (S1)}-\text{(S27)},\text{(S29)}-\text{(S31)}, \\ & \text{(S33)}-\text{(S122)} \\ & \text{energy balance constraints (S123)}-\text{(S126)} \\ & \text{economic evaluation constraints (1)}-\text{(3)}, \text{(10)}-\text{(18)} \\ & \text{environmental impact constraints (19)}-\text{(23)} \\ & \text{linearization constraints (24)}-\text{(35)} \end{aligned} \tag{P2}$$

5.2. Branch-and-Refine Algorithm. According to the linearization techniques utilized, the objective function value of problem P2 is an underestimator of that of problem P1. We apply a tailored branch-and-refine algorithm to solve this optimization problem.[48−50]

The algorithm starts by assigning the upper bound as positive infinity and the lower bound as zero. Then we approximate the original concave and convex power functions respectively with the initial segments and tangents to formulate the initial (P2). The MILP relaxed problem (P2) can be solved efficiently by the state-of-the-art branch-and-cut methods implemented in solvers such as CPLEX. The new upper bound is determined as the smaller one between the feasible objective function value of (P1) and the previous upper bound; the lower bound is selected as the larger one of the optimal objective function value of (P2) and the existing lower bound. If the gap between the upper bound and the lower bound is not smaller than the optimality tolerance, the algorithm will proceed to the next iteration. Following the optimal solution of problem P2, a new partition point can be generated in the corresponding interval and the piecewise linear approximation function can be refined by reevaluating the linear function parameters of each segment. After the new piecewise linear approximation function is formulated, the MILP problem (P2) is solved again. The updating procedure of the upper bound and the lower bound is similar to the first iteration.

As the iteration number increases, the number of intervals and partition points increase in (P2) and the best upper bound decreases while the best lower bound increases. As more pieces are added to approximate the original power function, the piecewise linear approximation will be more accurate. It deserves attention that the number of added partition points is not necessarily equal to the number of iterations, because if the optimal solutions are close enough to the bounds of the intervals in some iteration, we do not add new intervals or partition points to the existing relaxation problem (P2). If the upper bound and lower bound are close enough to reach the optimality tolerance, the algorithm will stop iterating and return the global optimal solution. The algorithm only requires an MILP solver, whereas a nonlinear programming solver can also be used to solve the upper bounding problem which fixes all the binary variables as the optimal solution value. Although simple function evaluation in updating the upper bound may reduce the solution quality, the computational efficiency is much higher. The flowchart of the branch-and-refine algorithm is summarized in Figure 6.

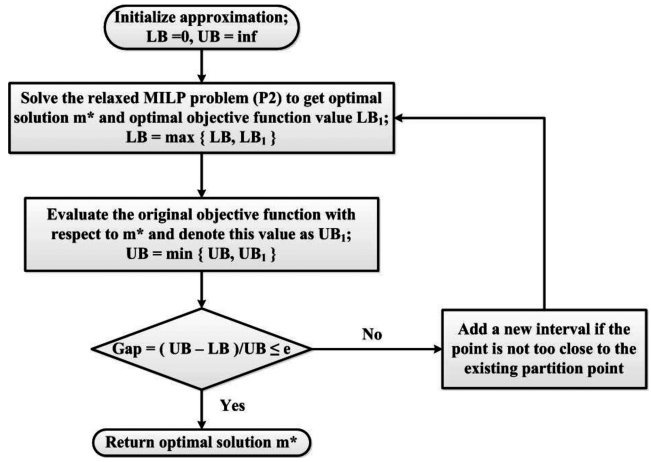

Figure 6. Flowchart of branch-and-refine algorithm.

6. RESULTS AND DISCUSSION

As a result of sequestrating carbon dioxide emissions from the upstream coal-fired power plant during both day and night, a large expense is constructing huge gasholders or providing a substantial amount of power for artificial LED light in this process superstructure. For the sake of establishing a cost-effective algal biorefinery for biological carbon sequestration and utilization, the possibility of feed gas delivery restricted during the day is examined as a special case of the original process. The special case does not involve night production decisions, and the associated investment cost is potentially reduced. Correspondingly, the superstructure is shown in Figure 7, and the border of continuous and discontinuous sections is redefined to cover the feed gas. Additionally, a permanent gasholder becomes necessary

dx.doi.org/10.1021/ie403459m | Ind. Eng. Chem. Res. 2014, 53, 1563−1579

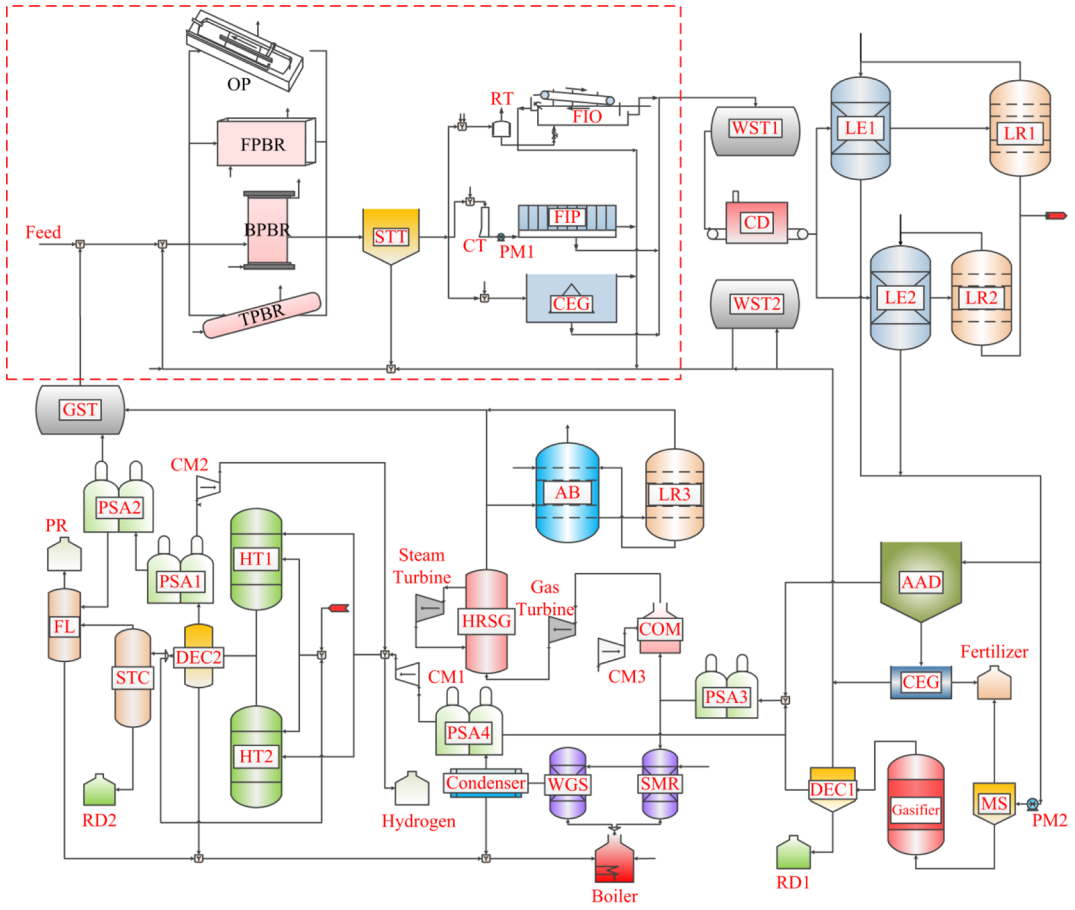

Figure 7. Superstructure for feed gas delivery only during the day. (Please refer to Figure 3 for the abbreviations.)

to hold recycled carbon dioxide produced from downstream processes at night.

All of the computational experiments are performed on a Dell Optiplex 790 desktop equipped with an Intel Core i5-2400 3.10 GHz CPU, 8 GB RAM, and Windows 7 64-bit operating system. The proposed MINLP problem is coded in GAMS 24.1.2. Furthermore, the MINLP problems (P1) are solved using BARON 12.3.3.[51] The MILP problems (P2) employing branch-and-refine algorithm are solved with CPLEX 12.5.1.0. The optimality tolerance for the branch-and-refine algorithm is set to 10^{-6}, and optimality margins of the solving original problem (P1) and the linear relaxation problem (P2) are both zero. Model statistics is summarized in Table 2.

6.1. Computational Performance. The computational performance of different methods for both the original case and the special case are compared in Table 3. BARON 12.3.3 did not return any feasible solutions for either case within 2 h. Nevertheless, the proposed branch-and-refine algorithm has a significantly better performance and the optimization problems were solved to global optimality effectively and efficiently. It takes only a few CPU seconds on average to iteratively solve the relaxed MILP problems (P2) to obtain the global optimal solutions of the MINLP problem (P1). The computational results demonstrate the strong advantage of applying the proposed branch-and-refine algorithm to globally optimize the MINLP process superstructure optimization problems with nonconvex power functions in the objective function.

The change of bounds during the branch-and-refine algorithm to solve the superstructure optimization problem of point A in the original case is illustrated in Figure 8. As the iterations proceed, the upper bound evaluated with respect to the optimal solution of (P2) continues decreasing, while the lower bound, which is the optimal solution of the linear MILP problem (P2), continues increasing, until they are close enough to reach the stopping criterion. The gap between the upper bound and the lower bound in the first iteration is very large and both values are far from the global optimality, because the linear approximation by the initial secants and tangents deviates too much from the original power functions. In the second iteration, the upper bound does not change but the lower bound slightly increases as the result of the improvement in the piecewise linear approximation function (P2). The gap in the third iteration reduces to a significantly small number and the upper bound obtained is already the global objective function value owing to the effectiveness of partitioning the previous optimal solutions

Table 2. Problem Statistics

	original case		special case	
	orig MINLP problem (P1)	relaxed MILP problem (P2)[a]	orig MINLP problem (P1)	relaxed MILP problem (P2)[a]
no. discrete vars	40	66	18	44
no. continuous vars	3577	3603	2575	2601
no. constraints	4111	4218	2837	2944

[a]The model statistics of the relaxed MILP problem (P2) is for the first iteration.

dx.doi.org/10.1021/ie403459m | Ind. Eng. Chem. Res. 2014, 53, 1563−1579

Table 3. Computational Performance

			branch-and-refine algorithm			BARON 12.3.3			
	point	power plant size (MW)	obj function ($/ton of CO_2)	iter	CPU (s)	obj function ($/ton of CO_2)	CPU (s)	lower bound	upper bound
original case	A	300	33.65	4	3.31	NA	7200	−150.78	6.3×10^6
	B	2400	9.52	4	3.88	NA	7200	−33.56	7.9×10^5
special case	C	300	11.90	4	3.34	NA	7200	−223.44	6.2×10^6
	D	2400	−12.23	4	2.82	NA	7200	−48.59	7.7×10^5

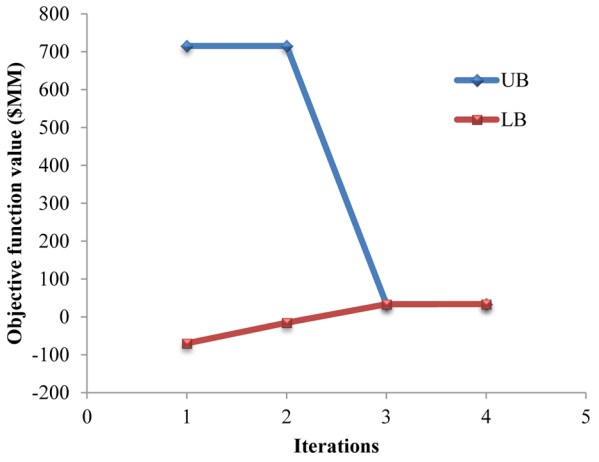

Figure 8. Upper and lower bounds of point A in each iteration in the original case.

into the feasible intervals to refine the linear approximation function (P2). Meanwhile, the lower bound keeps increasing and is rather close to the upper bound. In the last iteration, the gap is small enough to satisfy the termination criterion, so the algorithm stops and returns the global optimal solution.

6.2. Optimization Results. The relationships between minimum unit carbon sequestration and utilization cost and the size of the upstream coal-fired power plant in both the original and special cases are illustrated in Figure 9. The

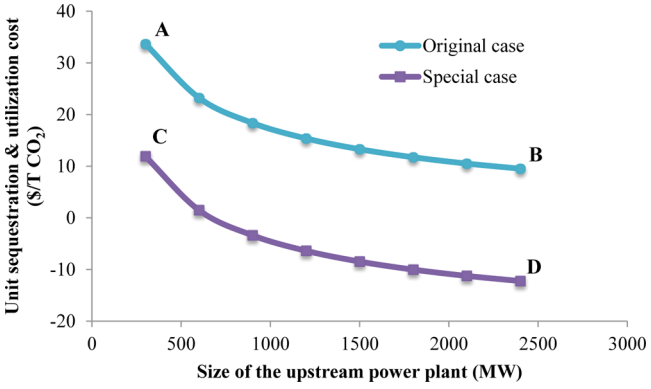

Figure 9. Optimal results of both cases when diesel sells at $3.91/gal.

horizontal axis is measured by comparing the annual sequestrated carbon dioxide amount in either case to the annual carbon dioxide emissions, 5,003.46 ktons, of a 600 MW coal-fired power plant.[52] We assume that the carbon dioxide emissions rate increases linearly with the size of the power plant. The vertical axis is the objective function in both the MINLP problem (P1) and the relaxed linear MILP problem (P2). Each point stands for an optimal process design when the relating carbon dioxide flow rate is considered, so the area below the curve is infeasible and the unit sequestration and utilization costs above the curve are feasible. The optimal unit sequestration cost decreases when the size of the upstream coal-fired power plant increases. The trend is due to the economy of scale, which is mathematically defined by power functions in capital cost evaluation. More details about the annualized investment cost and operating cost can be found in Figures 10 and 11. Both figures indicate that the annual operating

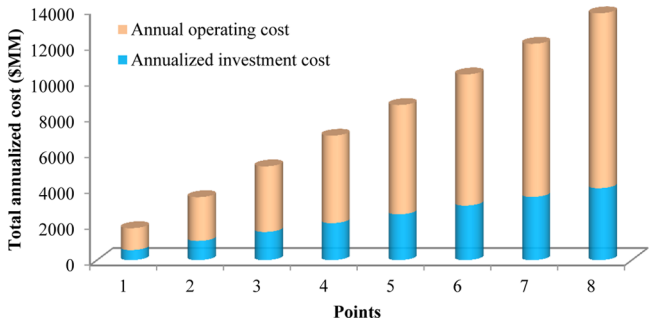

Figure 10. Annualized cost distribution in the original case when diesel price is $3.91/gal.

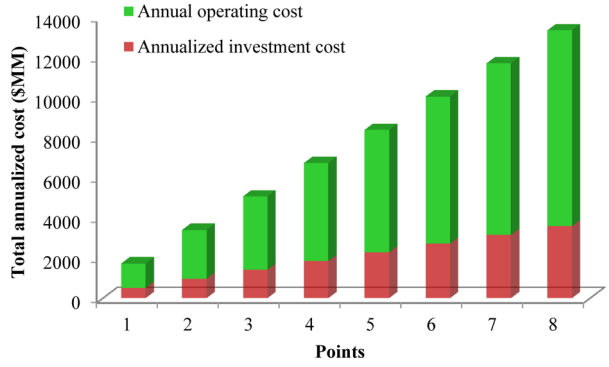

Figure 11. Annualized cost distribution in the special case when diesel price is $3.91/gal.

cost increases linearly, but the increment of annualized investment cost slows down when the size of the upstream coal-fired power plant expands.

The most recent investigation indicates diesel sells at $3.91 per gallon on average,[53] so most of our discussions are based on the optimization results at this price. Point A located on the curve of the original case demands $33.65 to sequestrate 1 ton of carbon dioxide for a 300 MW coal-fired power plant. In comparison, if the capacity of the algal biorefinery increases by 8 times, which is the case of point B, the unit sequestration cost will drop 71.71% to merely $9.52/ton of carbon dioxide sequestrated.

The optimal design of point B is illustrated in Figure 12. This design includes gas storage during the night, an open pond for algae cultivation, flotation thickening in advanced dehydration,

dx.doi.org/10.1021/ie403459m | Ind. Eng. Chem. Res. 2014, 53, 1563−1579

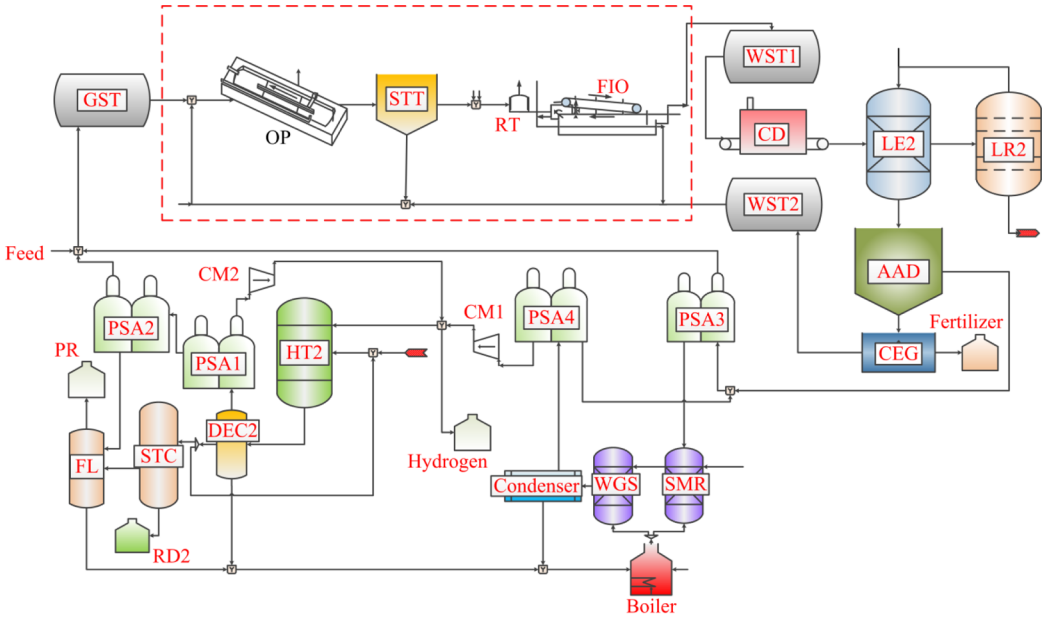

Figure 12. Optimal design of the algal superstructure of point B. (Please refer to Figure 3 for the abbreviations.)

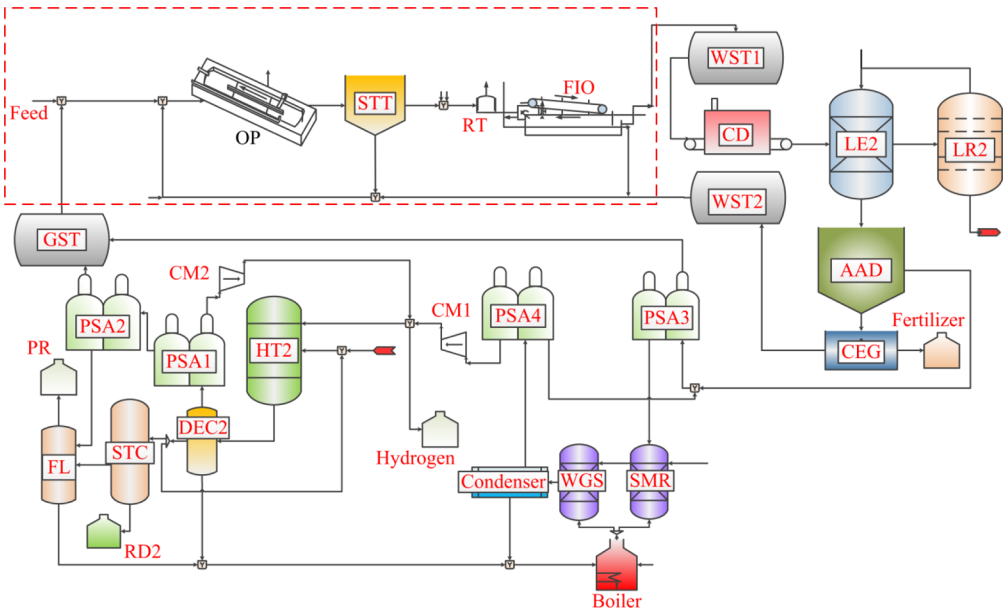

Figure 13. Optimal design of the algal superstructure of point D. (Please refer to Figure 3 for the abbreviations.)

1-butanol as the solvent in the lipid extractor, anaerobic digestion to break down the algae remnant, hydrogen production for biogas utilization, and finally Ni−Mo catalyst in the algal oil upgrading reactor. According to most existing algae-to-biofuel process evaluations, closed photobioreactors provide high productivity and stable production yield, but their high equipment cost and electricity consumption inevitably result in much higher budgets for investors. The economically optimal design selects flotation thickening, 1-butanol, and anaerobic digestion because they are less expensive to build and consume less energy. Biogas to hydrogen production is selected because the income of selling extra renewable oil cannot offset the investment cost of building a set of combustion facilities at such a production scale. Ni−Mo catalyst demonstrates better performance in producing valuable renewable diesel, so it is more suitable for a design with an economic objective. One issue deserving attention is that the selection of off-gas purification does not appear in the result because biogas is sent to steam reforming for hydrogen production, so no off-gas is produced from biogas combustion.

For the special case, point C requires \$11.90/ton of CO_2 sequestrated when the annual sequestrated quantity of this algal biorefinery equals the annual carbon dioxide emissions of a 300 MW coal-fired power plant. Since the captured carbon dioxide is not delivered to the algal biorefinery at night, the actual feed gas flow rate during the day equals the carbon dioxide emission rate of a 600 MW coal-fired power plant. Surprisingly, for point D to sequestrate 1 ton of carbon dioxide when the annual sequestrated quantity balances the emissions of a 2400 MW coal-fired power plant, the biorefinery earns \$12.23/ton of CO_2 sequestrated. In fact, the biorefinery starts to make a profit when the size of the corresponding power plant exceeds 700 MW. Furthermore, with

dx.doi.org/10.1021/ie403459m | Ind. Eng. Chem. Res. 2014, 53, 1563−1579

the larger size of the power plant or the higher flow rate of feed gas, more profit will be made. As shown in Figure 13, the optimal design for point D is rather similar to the design of point B, requiring an open pond for algae cultivation, flotation in advanced dehydration, 1-butanol as the solvent in the lipid extraction section, anaerobic digestion to break down the algae remnant, hydrogen production for biogas utilization, and finally Ni−Mo catalyst in algal oil upgrading facilities.

Given the same diesel price and annual carbon sequestration and utilization quantity, the special case demonstrates lower unit sequestration and utilization cost than the original case as shown in Figure 9. More details about the cost superiority of the special case are revealed from Figures 14 and 15. If both cases receive the

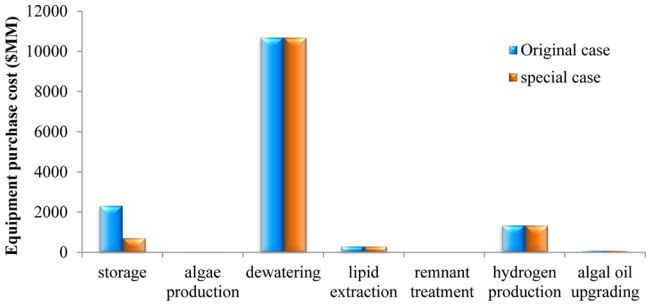

Figure 14. Equipment purchase cost distribution of both cases.

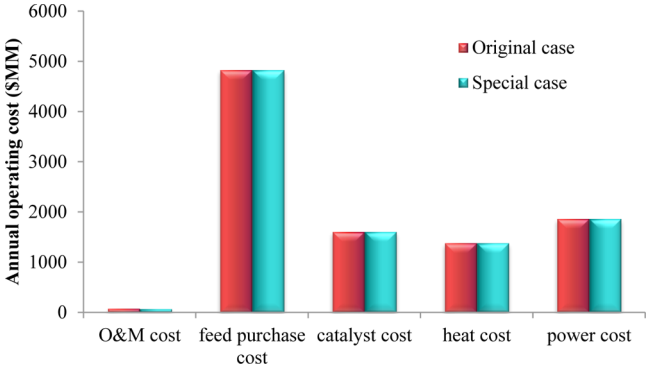

Figure 15. Annual operating cost distribution of both cases.

same amount of feed gas for sequestration in a year, the optimal solution of the original case will select to reserve all feed gas at night to be used in the next day's production, which accords with the production conditions in the special case that the carbon dioxide is transported and absorbed by algae only during the day. Therefore, the production and downstream upgrading facilities require the same production conditions in both cases and the only difference lies in a higher capital cost of building the gasholder for the original case. Other than the higher capital cost, the huge volume of the gasholders which contain all the feed gas during the night is difficult for both construction and arrangement.

The distributions of the annual operating cost of both cases are provided in Figure 15. The operation and maintenance (O&M) cost, feed purchase cost, catalyst cost, heat supply cost, and power consumption cost account for about 1, 49, 17, 14 and 19%, respectively. The original case differs from the special one only in the O&M cost, which is evaluated by a percentage of the total investment cost. The major contribution of the operating cost comes from the feedstock purchase cost, whose specific distribution is shown in Figure 16. In both optimal process

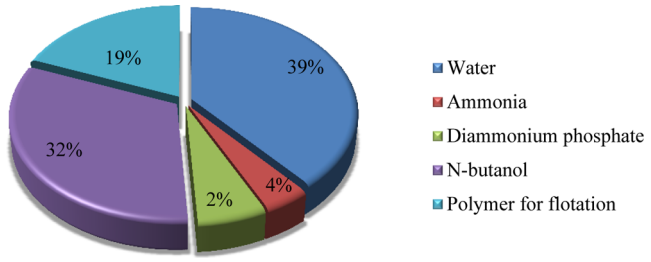

Figure 16. Feedstock purchase cost distribution for both cases.

designs, the open pond is selected as the bioreactor to cultivate algae and water evaporates at a fast rate of 570 gal/gal lipid[15] due to direct exposure to the atmosphere. Even though the price of water is extremely low, large amount of water loss leads to 39% of the total operating cost. 1-Butanol is selected as the solvent in the lipid extractor and a solvent-to-algae ratio of 5:1 is adopted to ensure adequate mixing, so that make-up 1-butanol, which contributes to 32% of the entire operating cost, is important to balance the loss of solvent in lipid stream.

Figure 17 presents the direct and indirect life cycle environmental performances of the algal biorefinery in both

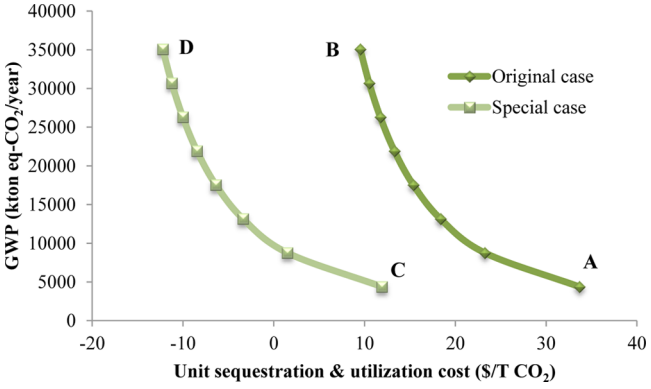

Figure 17. Environmental performance of both cases.

cases with respect to the minimum unit sequestration and utilization cost. The horizontal axis is the unit sequestration and utilization cost, and the vertical axis is the GWP. In both cases, GWP of the algal biorefinery increases when the unit sequestration and utilization cost of the corresponding biorefinery decreases. For points A and C with the same sequestration amount equivalent to a 300 MW coal-fired power plant, their GWPs are both 4385.44 ktons of CO_2 equiv/year. Due to larger heat and power consumption for operation, the GWP increases to 35 083.45 ktons of CO_2 equiv/year for both points B and D. Consequently, the special case demonstrates clear environmental benefits over the original case when the unit CO_2 sequestration and utilization cost is fixed.

Judged from both economic and environmental behaviors, the optimal design from the special case is superior to that in the original case. According to some reports from the open literature,[54] the unit storage cost with respect to geological methods ranges from \$0.5/ton to \$8/ton of carbon dioxide sequestrated depending on the specific technology and carbon dioxide flow rate, storage type, depth, and geological characteristics of the intended location. If the upstream coal-fired power plant is greater than 660 MW, the optimal unit sequestration and utilization cost of algal biorefinery through the biological carbon

dx.doi.org/10.1021/ie403459m | Ind. Eng. Chem. Res. 2014, 53, 1563−1579

sequestration pathway, ranging from $−12.23 to $11.90 in the special case, will be lower than its competitors.

However, one may point out that the low unit sequestration cost of the special case is estimated with the prerequisite that captured carbon dioxide is delivered to the algal biorefinery only during the day, but every power plant operates continuously and the flue gas emits 24 hours a day. This deficiency can be handled by integrating multiple sequestration approaches: the algal biorefinery takes care of the carbon emission during the day and geological sequestration stores the carbon dioxide produced at night. The geological sequestration method benefits from a larger sequestration capacity, while the algal biorefinery takes advantage of flexibility in choosing the plant location and expanding the production scale. If the cooperation between these technologies is realized, the overall carbon sequestration process will be more economically viable and appropriate for future practice.

6.3. Sensitivity Analysis. Among all parameters, diesel price is one of the most important factors that determine the economic performance of this algal biorefinery. However, it varies frequently and depends largely on international and domestic markets. Recent statistics show that the average petroleum-derived diesel price is $3.91/gal and the biodiesel price (B100) is $4.19/gal. Accordingly, we set up another assumed lower price of $3.63/gal for the sensitivity analysis. Figures 18 and 19 show the

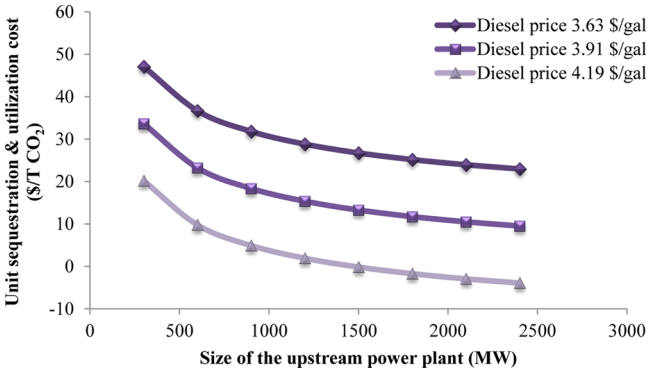

Figure 18. Minimized unit CO_2 sequestration and utilization cost in the original case.

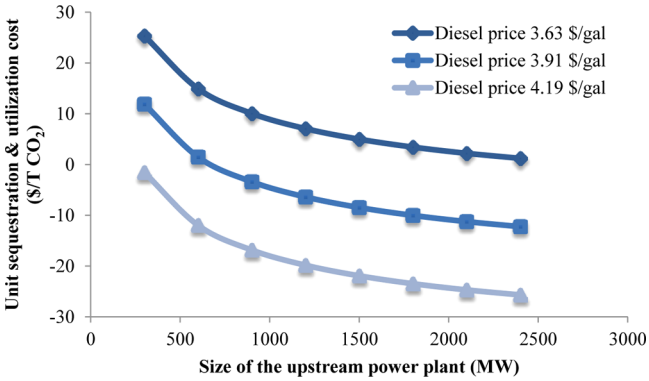

Figure 19. Minimized unit CO_2 sequestration cost utilization in the special case.

unit sequestration cost at different diesel market prices in the original case and the special case, respectively. A higher diesel market price brings more credit to offset the total cost, so it results in a lower unit cost of biological carbon dioxide sequestration and utilization. There are no turning points occurring, so that the change of price is not big enough to make a switch in technology selection. Furthermore, following the rise of price, the unit carbon sequestration cost decreases more and more significantly when the size of the upstream coal-fired power plant increases. If the price increases by 7.71% from $3.63 to $3.91, the percentage of change of unit sequestration and utilization cost will increase from 28.56 to 58.56% in the original case. This can be explained by the following: rising price to a small extent purely offsets a portion of investment cost and the unit cost drop is a fixed value related to the change of price. As a result, the proportion of this fixed value to the decreasing unit sequestration cost naturally becomes larger and larger.

Similarly, diesel price plays an important role in influencing the unit sequestration price in the special case. If the diesel price rises from $3.63/gal to $4.19/gal, the algal biorefinery makes a profit from biological carbon sequestration for whatever size of the upstream coal-fired power plant is considered on the curve.

7. CONCLUSION

In this work we proposed a strengthened superstructure of algal biorefinery processes for biological carbon sequestration and utilization. The algal biorefinery constituted seven major sections: off-gas purification, algae cultivation, harvesting and dewatering, lipid extraction, remnant treatment, biogas utilization, and algal oil upgrading. Each section considered multiple technology alternatives including the selections between direct or purified off-gas; among open pond, flat plate photobioreactor, bubble column photobioreactor, and tubular photobioreactor; among flotation thickening, filtration, and centrifugation dewatering technologies; of hexane or 1-butanol for extraction solvent; of anaerobic digestion or catalytic gasification in remnant treatment; of hydrogen production or direct combustion of biogas; and of Co−Mo or Ni−Mo as the catalyst in the hydrotreating reactor. Accordingly, we proposed a rigorous MINLP optimization model for this process superstructure to minimize the unit CO_2 sequestration and utilization cost subject to mass balance constraints, energy balance constraints, technoeconomic constraints, and LCA constraints. As the MINLP model included nonconvex nonlinear terms, we applied a tailored branch-and-refine algorithm based on successive piecewise linear approximation to globally optimize the superstructure optimization model within a reasonable computational time.

The optimization results indicate that if carbon dioxide is delivered to the algal biorefinery 24 hours a day, the optimal unit CO_2 sequestration and utilization cost will reduce from $33.65/ton of CO_2 to $9.52/ton of CO_2 when the size of the upstream power plant expands from 300 to 2400 MW. If the feed gas is limited only during the day, the optimal unit sequestration and utilization cost ranges from $11.90/ton of CO_2 to $−12.23/ton of CO_2 correspondingly. All the optimal results of the original case select to store feed gas delivered at night in a temporary storage device other than to continue production using artificial light. Therefore, the only difference between these two cases is the volume of the storage device. The optimal design when the diesel prices is $3.91/gal and feed gas is delivered to the biorefinery only during daytime at a flow rate of 5003.46 ktons/year corresponding to the carbon dioxide emission rate of a 600 MW coal-fired power plant requires a unit cost of $1.48/ton of CO_2 and selects open pond, flotation thickening, 1-butanol solvent extraction, anaerobic digestion, biogas utilized to produce hydrogen, and Ni−Mo as the catalyst in algal oil upgrading reactor. Further sensitive analysis upon the product

dx.doi.org/10.1021/ie403459m | Ind. Eng. Chem. Res. 2014, 53, 1563−1579

selling price demonstrates that a higher diesel price results in lower unit sequestration and utilization cost.

■ ASSOCIATED CONTENT

Supporting Information

The mathematical formulation (including (S1)−(S126)) and related data. This material is available free of charge via the Internet at http://pubs.acs.org.

■ AUTHOR INFORMATION

Corresponding Author

*E-mail: you@northwestern.edu. Tel.: (847) 467-2943. Fax: (847) 491-3728; .

Notes

The authors declare no competing financial interest.

■ ACKNOWLEDGMENTS

The authors are grateful to Randall Waymire for his help in developing the process superstructure. The financial support from the Institute for Sustainability and Energy at Northwestern University (ISEN) is gratefully acknowledged.

■ NOMENCLATURE

Sets

IP = set of LED irradiance candidate
J = set of all species involved in the process
CCT = set of off-gas purification technologies
TIME = set of time
AGT = set of algae growth technologies
HTT = set of technologies for hydroprocessing
JDFG = set of gas stored in the gasholder
L = set of units for economic evaluation
L1 = set of units for heat consumption
L2 = set of units for power consumption
L3 = set of units in economic evaluation using sizing method
L4 = set of feed to purchase
L5 = set of products
P = set of partition intervals in piecewise approximation

Variables

$m^i_{k,j}$ = mass flow rate of species j of stream i in alternative technology k, tons/h
V_{agt} = volume of bioreactor agt, $10^3 m^3$
$\text{productivity}^{night}_{agt}$ = productivity of technology agt during night, $kg/m^3/h$
$\omega_{agt,ip}$ = transformation variable of $yprod_{agt,ip} V_{agt}$, 10^3 m^3
Q_g = heat generation from condenser, MW
Q^{l1}_c = heat consumption of unit l1, MW
E_g = power generation from gas turbine and steam turbine system, MW
E^{l2}_c = power consumption of unit l2, MW
CC_l = capital cost of unit l, $MM
TIC = total investment cost, $MM
AIC = annualized investment cost, $MM
FPC = feed purchase cost, $MM
STMC = steam cost, $MM
PC = power cost, $MM
OMC = operation and maintenance cost, $MM
AOC = annualized operation cost, $MM
TAC = total annualized cost, $MM
OBJ = objective function, unit biological sequestration and utilization cost, $/ton of CO_2
LCI^{emiss}_j = life cycle inventory of species j as direct emission, tons/year
GWP^i = global warming potential of item i, ktons equiv CO_2/year
GWP = total global warming potential, ktons equiv CO_2/year
$yprod_{agt,ip}$ = binary varible to determine candidate ip of bioreactor agt
y_p = binary varible to determine the piecewise linear approximation intervals

Parameters

UB = upper bound of the capacity, tons
T_{time} = hours during time, h
$\text{pproductivity}^{day}_{agt}$ = productivity of technology agt during the day, $kg/m^3/h$
$\text{pproductivity}^{night}_{agt,ip}$ = productivity candidate ip of technology agt during night, $kg/m^3/h$
$\text{pI}^{night}_{agt,ip}$ = LED intensity candidate ip of technology agt during night, $\mu mol/m^2/s$
f^b_{l3} = base-case mass flow rate of interested species in l3, tons/h
CC^b_{l3} = base-case capital cost of interested species in l3, $MM
sf_{l3} = sizing factor of l3
$CEPCI_{l3}$ = chemical engineering plant cost index of l3 at present value
$CEPCI^{ref}_{l3}$ = chemical engineering plant cost index of l3 of the reference year
K_{eng} = factor of engineering cost
K_{lg} = factor of legal and contractors cost
K_{ctg} = factor of project contingency cost
K_{wcp} = factor of working capital cost
ir = interest rate
lifespan = life span of the algal biorefinery, years
$Price_j$ = market price of j, $/kg
K_{OM} = factor of operation and maintenance cost
ϕ_j = damage factor that accounts for gwp associated with species j, kg equiv CO_2/kg
θ^{pc} = damage factor per unit energy of power, kg equiv CO_2/kWh
θ^{hc} = damage factor per unit energy of heat, kg equiv CO_2/kWh

Subscripts/Superscripts

wr = water
cdo = carbon dioxide
nit = nitrogen
oxy = oxygen
MEA = monoethanolamine
C = carbon element
N = nitrogen element
P = phosphorus element
al = algae
lip = lipid
rem = remnant
met = methane
hyd = hydrogen
cmo = carbon monoxide
ext = extraction
aad = anaerobic digestion
hp = hydrogen production
hdp = hydroprocessing
ag = algae growth
cd = cell disrupture
cg = catalytic gasification
fer = fertilizer

emiss = emission

REFERENCES

(1) Ferrell, J.; Sarisky-Reed, V. *National Algal Biofuels Technology Roadmap*; U.S. Department of Energy: College Park, MD, 2010.

(2) Yue, D.; You, F.; Snyder, S. W. Biomass-to-bioenergy and biofuel supply chain optimization: Overview, key issues and challenges. *Comput. Chem. Eng.* **2014**, DOI: 10.1016/j.compchemeng.2013.11.016.

(3) Brennan, L.; Owende, P. Biofuels from microalgae—A review of technologies for production, processing, and extractions of biofuels and co-products. *Renewable Sustainable Energy Rev.* **2010**, *14* (2), 557−577.

(4) Chisti, Y. Biodiesel from microalgae. *Biotechnol. Adv.* **2007**, *25* (3), 294−306.

(5) Mata, T. M.; Martins, A. A.; Caetano, N. S. Microalgae for biodiesel production and other applications: A review. *Renewable Sustainable Energy Rev.* **2010**, *14* (1), 217−232.

(6) Martin, M.; Grossmann, I. E. Optimal engineered algae composition for the integrated simultaneous production of bioethanol and biodiesel. *AIChE J.* **2013**, *59* (8), 2872−2883.

(7) Martin, M.; Grossmann, I. E. Simultaneous Optimization and Heat Integration for Biodiesel Production from Cooking Oil and Algae. *Ind. Eng. Chem. Res.* **2012**, *51* (23), 7998−8014.

(8) Baliban, R. C.; Elia, J. A.; Floudas, C. A.; Gurau, B.; Weingarten, M. B.; Klotz, S. D. Hardwood Biomass to Gasoline, Diesel, and Jet Fuel: 1. Process Synthesis and Global Optimization of a Thermochemical Refinery. *Energy Fuels* **2013**, *27* (8), 4302−4324.

(9) Chen, Y.; Li, X.; Adams, T. A.; Barton, P. I. Decomposition strategy for the global optimization of flexible energy polygeneration systems. *AIChE J.* **2012**, *58* (10), 3080−3095.

(10) Liu, P.; Pistikopoulos, E. N.; Li, Z. Decomposition Based Stochastic Programming Approach for Polygeneration Energy Systems Design under Uncertainty. *Ind. Eng. Chem. Res.* **2010**, *49* (7), 3295−3305.

(11) Gebreslassie, B. H.; Waymire, R.; You, F. Sustainable design and synthesis of algae-based biorefinery for simultaneous hydrocarbon biofuel production and carbon sequestration. *AIChE J.* **2013**, *59* (5), 1599−1621.

(12) Wang, B.; Gebreslassie, B. H.; You, F. Q. Sustainable design and synthesis of hydrocarbon biorefinery via gasification pathway: Integrated life cycle assessment and technoeconomic analysis with multiobjective superstructure optimization. *Comput. Chem. Eng.* **2013**, *52*, 55−76.

(13) Gebreslassie, B. H.; Slivinsky, M.; Wang, B. L.; You, F. Q. Life cycle optimization for sustainable design and operations of hydrocarbon biorefinery via fast pyrolysis, hydrotreating and hydrocracking. *Comput. Chem. Eng.* **2013**, *50*, 71−91.

(14) Zhang, Q.; Gong, J.; Skwarczek, M.; Yue, D.; You, F. Sustainable process design and synthesis of hydrocarbon biorefinery through fast pyrolysis and hydroprocessing. *AIChE J.* **2013**, DOI: 10.1002/aic.14344.

(15) Davis, R.; Aden, A.; Pienkos, P. T. Techno-economic analysis of autotrophic microalgae for fuel production. *Appl. Energy* **2011**, *88* (10), 3524−3531.

(16) Davis, R.; Aden, A. *Renewable Diesel from Algal Lipids: An Integrated Baseline for Cost, Emissions, and Resource Potential from a Harmonized Model*; Argonne National Laboratory: Argonne, IL, 2012.

(17) Frank, E.; Han, J.; Palou-Rivera, I.; Elgowainy, A.; Wang, M. *Life-Cycle Analysis of Algal Lipid Fuels with the GREET Model*; Center for Transportation Research, Energy Systems Division, Argonne National Laboratory, Argonne, IL, 2011.

(18) Pokoo-Aikins, G.; Nadim, A.; El-Halwagi, M. M.; Mahalec, V. Design and analysis of biodiesel production from algae grown through carbon sequestration. *Clean Technologies and Environmental Policy* **2010**, *12* (3), 239−254.

(19) Sun, A.; Davis, R.; Starbuck, M.; Ben-Amotz, A.; Pate, R.; Pienkos, P. T. Comparative cost analysis of algal oil production for biofuels. *Energy* **2011**, *36* (8), 5169−5179.

(20) Lundquist, T. J.; Woertz, I. C.; Quinn, N.; Benemann, J. R. A realistic technology and engineering assessment of algae biofuel production. *Energy Biosci. Inst.* **2010**, 1.

(21) Fisher, K.; Beitler, C.; Rueter, C.; Searcy, K.; Rochelle, G.; Jassim, M. *Integrating MEA Regeneration with CO2 Compression and Peaking to Reduce CO2 Capture Costs—Final Report*. U.S. Department of Energy, National Energy Technology Laboratory: Pittsburgh, PA, 2005.

(22) Alabi, A. O.; Bibeau, E.; Tampier, M. *Microalgae Technologies & Processes for Biofuels—Bioenergy Production in British Columbia: Current Technology, Suitability & Barriers to Implementation: Final Report*; British Columbia Innovation Council: Vancouver, BC, 2009.

(23) Sierra, E.; Acien, F. G.; Fernandez, J. M.; Garcia, J. L.; Gonzalez, C.; Molina, E. Characterization of a flat plate photobioreactor for the production of microalgae. *Chem. Eng. J.* **2008**, *138* (1−3), 136−147.

(24) Zhang, C. W.; Zmora, O.; Kopel, R.; Richmond, A. An industrial-size flat plate glass reactor for mass production of Nannochloropsis sp (Eustigmatophyceae). *Aquaculture* **2001**, *195* (1−2), 35−49.

(25) Molina, E.; Fernandez, J.; Acien, F. G.; Chisti, Y. Tubular photobioreactor design for algal cultures. *J. Biotechnol.* **2001**, *92* (2), 113−131.

(26) Fernandez, F. G. A.; Sevilla, J. M. F.; Perez, J. A. S.; Grima, E. M.; Chisti, Y. Airlift-driven external-loop tubular photobioreactors for outdoor production of microalgae: assessment of design and performance. *Chem. Eng. Sci.* **2001**, *56* (8), 2721−2732.

(27) Miron, A. S.; Camacho, F. G.; Gomez, A. C.; Grima, E. M.; Chisti, Y. Bubble-column and airlift photobioreactors for algal culture. *AIChE J.* **2000**, *46* (9), 1872−1887.

(28) Grima, E. M.; Fernandez, F. G. A.; Camacho, F. G.; Chisti, Y. Photobioreactors: light regime, mass transfer, and scaleup. *J. Biotechnol.* **1999**, *70* (1−3), 231−247.

(29) Wang, C. Y.; Fu, C. C.; Liu, Y. C. Effects of using light-emitting diodes on the cultivation of Spirulina platensis. *Biochem. Eng. J.* **2007**, *37* (1), 21−25.

(30) McMillan, J. R.; Watson, I. A.; Ali, M.; Jaafar, W. Evaluation and comparison of algal cell disruption methods: Microwave, waterbath, blender, ultrasonic and laser treatment. *Appl. Energy* **2013**, *103*, 128−134.

(31) Bradshaw, S. M.; van Wyk, E. J.; de Swardt, J. B. Microwave heating principles and the application to the regeneration of granular activated carbon. *J. S. Afr. Inst. Min. Metall.* **1998**, *98* (4), 201−210.

(32) Bollmeier, W.; Sprague, S.; No, F. *Aquatic Species Program*; Solar Energy Research Institute: Golden, CO, 1989.

(33) Collet, P.; Helias, A.; Lardon, L.; Ras, M.; Goy, R. A.; Steyer, J. P. Life-cycle assessment of microalgae culture coupled to biogas production. *Bioresour. Technol.* **2011**, *102* (1), 207−214.

(34) Elliott, D. C.; Hart, T. R.; Neuenschwander, G. G.; Rotness, L. J.; Olarte, M. V.; Zacher, A. H. Chemical Processing in High-Pressure Aqueous Environments. 9. Process Development for Catalytic Gasification of Algae Feedstocks. *Ind. Eng. Chem. Res.* **2012**, *51* (33), 10768−10777.

(35) Martin, M.; Grossmann, I. E. Energy optimization of hydrogen production from lignocellulosic biomass. *Comput. Chem. Eng.* **2011**, *35* (9), 1798−1806.

(36) Albrecht, K. O.; Hallen, R. T. *A Brief Literature Overview of Various Routes to Biorenewable Fuels from Lipids for the National Alliance for Advanced Biofuels and Bio-products (NAABB) Consortium*; Pacific Northwest National Laboratory: Richland, WA, 2011.

(37) Marker, T. *Opportunities for Biorenewables in Oil Refineries*; UOP LLC: Des Plaines, IL, 2005.

(38) Seider, W. D.; Seader, J. D.; Lewin, D. R. *Product & Process Design Principles: Synthesis, Analysis and Evaluation* [CD-ROM]; Wiley: New York, 2009.

(39) California Stormwater QualityAssociation. *California Stormwater BMP Handbook—New Development and Redevelopment*; California Stormwater Quality Association: Menlo Park, CA, 2003.

(40) Lozowski, D. Chemical engineering plant cost index (CEPCI). *Chem. Eng.* **2012**, *119*, 84.

(41) Yue, D. J.; Kim, M. A.; You, F. Q. Design of Sustainable Product Systems and Supply Chains with Life Cycle Optimization Based on Functional Unit: General Modeling Framework, Mixed-Integer Nonlinear Programming Algorithms and Case Study on Hydrocarbon Biofuels. *ACS Sustainable Chem. Eng.* **2013**, *1* (8), 1003−1014.

(42) You, F. Q.; Tao, L.; Graziano, D. J.; Snyder, S. W. Optimal design of sustainable cellulosic biofuel supply chains: Multiobjective optimization coupled with life cycle assessment and input-output analysis. *AIChE J.* **2012**, *58* (4), 1157−1180.
(43) You, F. Q.; Wang, B. Life Cycle Optimization of Biomass-to-Liquid Supply Chains with Distributed-Centralized Processing Networks. *Ind. Eng. Chem. Res.* **2011**, *50* (17), 10102−10127.
(44) Glover, F. Improved Linear Integer Programming Formulations of Nonlinear Integer Problems. *Manage. Sci.* **1975**, *22* (4), 455−460.
(45) Padberg, M. Approximating separable nonlinear functions via mixed zero-one programs. *Oper. Res. Lett.* **2000**, *27* (1), 1−5.
(46) Croxton, K. L.; Gendron, B.; Magnanti, T. L. A comparison of mixed-integer programming models for nonconvex piecewise linear cost minimization problems. *Manage. Sci.* **2003**, *49* (9), 1268−1273.
(47) Quesada, I.; Grossmann, I. E. A global optimization algorithm for linear fractional and bilinear programs. *J. Global Optim.* **1995**, *6* (1), 39−76.
(48) You, F. Q.; Grossmann, I. E. Stochastic Inventory Management for Tactical Process Planning Under Uncertainties: MINLP Models and Algorithms. *AIChE J.* **2011**, *57* (5), 1250−1277.
(49) You, F. Q.; Pinto, J. M.; Grossmann, I. E.; Megan, L. Optimal Distribution-Inventory Planning of Industrial Gases. II. MINLP Models and Algorithms for Stochastic Cases. *Ind. Eng. Chem. Res.* **2011**, *50* (5), 2928−2945.
(50) Yue, D.; You, F. Planning and scheduling of flexible process networks under uncertainty with stochastic inventory: MINLP models and algorithm. *AIChE J.* **2013**, *59* (5), 1511−1532.
(51) Tawarmalani, M.; Sahinidis, N. V. A polyhedral branch-and-cut approach to global optimization. *Math. Program.* **2005**, *103* (2), 225−249.
(52) NineSigma. Technology To Reduce Flue Gas Emissions from Existing Power Plants. https://www.myninesigma.com/_layouts/RFPs/NineSigma_RFP_67698.pdf.
(53) DOE. Fuel Prices. http://www.afdc.energy.gov/fuels/prices.html.
(54) Metz, B.; Davidson, O.; de Coninck, H.; Loos, M.; Meyer, L.; Working Group III. *IPCC Special Report on Carbon Dioxide Capture and Storage*; Intergovernmental Panel on Climate Change: Geneva, Switzerland, 2005.